Whisker sensing by force and moment measurements at the whisker base

E. L. Starostin

School of Engineering, London South Bank University, 103 Borough Rd, London SE1 0AA, UK
and
Department of Civil, Environmental and Geomatic Engineering, University College London, Gower St, London WC1E 6BT, UK
E-mail: e.starostin@ucl.ac.uk

V. G. A. Goss

School of Engineering, London South Bank University, 103 Borough Rd, London SE1 0AA, UK
E-mail: gossga@lsbu.ac.uk

G. H. M. van der Heijden

Department of Civil, Environmental and Geomatic Engineering, University College London, Gower St, London WC1E 6BT, UK
E-mail: g.heijden@ucl.ac.uk

Abstract: We address the theoretical question which forces and moments measured at the base of a whisker (tactile sensor) allow for the prediction of the location in space of the point at which a whisker makes contact with an object. We deal with the general case of three-dimensional deformations as well as with the special case of planar configurations. All deformations are treated as quasi-static and contact is assumed to be frictionless. We show that the minimum number of independent forces or moments required is three but that conserved quantities of the governing elastic equilibrium equations prevent certain triples from giving a unique solution in the case of contact at any point along the whisker except the tip. The existence of these conserved quantities depends on the material and geometrical properties of the whisker. For whiskers that are tapered and intrinsically curved there is no obstruction to the prediction of the contact point. We show that the choice of coordinate system (Cartesian or cylindrical) affects the number of suitable triples. Tip and multiple point contact are also briefly discussed. Our results explain recent numerical observations in the literature and offer guidance for the design of robotic tactile sensory devices.

Keywords: Whisker, Tactile Sensor, Multiple Point Contact, Elastic Rod, Boundary-value Problem, Conserved Quantity.

1 Introduction

Whiskers (vibrissae) provide many animals with a sense of touch. These animals can use their whiskers to obtain information about geometrical and mechanical properties of their environment (see [1] and references therein). Animal whiskers are thin flexible rods grown out of follicles; there are no sensory nerve endings along the length of a whisker. Sensing therefore relies on the detection by mechanoreceptors at the whisker base of forces and moments induced by contact with an external object and transmitted through the elastic medium [2, 3].

Knowledge of how whiskers perform their sensory functions is of interest to engineers designing biomimetic tactile sensors [4, 5, 6, 7, 8, 9]. To use such artificial whiskers in robotics, it is often essential to be able to determine the location of the point along the whisker shaft at which contact with an object occurs.

We consider the quasi-static case, valid for sufficiently slow approach of the whisker to the object. Then, if three forces and three moments (in three independent spatial directions) are measured at the (fixed) whisker base, a suitable mechanical model of the whisker (e.g., a one-dimensional (1D) continuum elastic rod or beam model [10]) allows the entire configuration of the whisker to be determined. If it is furthermore assumed that the contact is frictionless then the location of the contact point can be obtained [7, 8, 9]. These six measurements, however, require an expensive six-axis load cell. It is natural, therefore, to ask whether fewer measurements

would suffice to uniquely predict the location of the contact point.

Past studies of this contact problem have mainly focussed on the planar case, where the contact point is specified by two coordinates [11, 7, 12, 13, 14]. Whisker configurations, especially those with intrinsic curvature, may generally be non-planar. In [15] the authors examine the 3D case, including whiskers with intrinsic curvature and taper. Using numerical simulation, they consider all 20 possible combinations of triples of base forces and moments. They report that certain triples uniquely predict the location of the contact point, but that other triples do not. They offer no theoretical explanation of this observation. Based on these results, in [16] an artificial whisker is constructed that operates by measuring the two bending moments and the axial force at the whisker base.

Here we show that the difference in the predictive ability of triples of forces and moments is mainly caused by the existence of conserved quantities of the differential equations governing the deformation of slender elastic bodies. These conserved quantities arise for whiskers with certain geometrical profiles (curvature, taper, etc.). We model whisker-object contact by formulating a two-point boundary-value problem using Kirchhoff rod theory [10]. Unlike (Euler-Bernoulli or Timoshenko) beam theory, this theory allows for arbitrarily large deformations of the whisker from its unstressed configuration. We will argue, however, that these model details are not essential for the predictability question, which is qualitative in nature.

We also consider the reconstruction problem for whiskers with multiple point contacts, which has seen recent interest. It was reported in [17] that 2D whisker configurations with two point contacts cannot be reconstructed from base measurements. Our results confirm and explain this observation and show that for 3D configurations reconstruction from base measurements is possible for whiskers with (at most) two point contacts.

We provide a theoretical explanation for experimental and numerical results on the ability to discriminate, by means of base measurements, between tip and non-tip contact of a whisker in a planar configuration having either one or two point contacts [22, 17]. We show that these results extend to 3D whisker configurations and to configurations with an arbitrary number of point contacts.

The organisation of the paper is as follows. In Section 2 we review well-posedness of boundary-value problems (BVPs) for (nonlinear) ordinary differential equations (ODEs) in the presence of conserved quantities. In Section 3 we introduce the BVP for tactile sensing by means of base measurements and identify its conserved quantities. This BVP is then analysed for its ability to predict the location of the (non-tip) contact point in Section 4. We also examine the special case of a planar sensing problem, more frequently studied in the literature, where two base measurements are sufficient (Section 5), and briefly consider the cases of tip contact (Section 6) and multiple contact (Section 7), both of which are easier to classify. Finally, in Section 8, we give an extensive discussion of our results.

2 Boundary-value problems and conserved quantities

The solution of an nth-order ODE, $du/ds = f(u)$, $u \in \mathbb{R}^n$, $s \in [a, b]$, involves n integration constants. Physical problems usually come with boundary conditions at $s = a$ and/or $s = b$, generally n conditions in the form $g(u(a), u(b)) = 0$, that fix these integration constants. In the special case of an initial-value problem, i.e., when all boundary conditions are specified at one end ($u(a) = c$ or $u(b) = c$, with c a given constant), there exists a unique solution (under very mild smoothness conditions on f). For general, two-point, BVPs, however, this is not guaranteed [18]. Non-uniqueness typically occurs as branch points (bifurcations) at special values of any parameters in f or g. An example of such non-uniqueness is encountered in differential equations with conserved quantities.

A conserved quantity (first integral) of an ODE is a function of the dependent variables u_i $(i = 1, ..., n)$ whose value is constant along solutions of the equation. The presence of such quantities may put constraints on the specification of boundary conditions: if conserved quantities are fixed by boundary conditions at one end they effectively add equations to the conditions $g = 0$ and therefore have to be compatible with them. For instance, in the simple case that one of the variables itself, say u_k, is a conserved quantity, the boundary condition $u_k(a) = c$, for some constant c, implies $u_k(b) = c$. Then $u_k(b) = d$ is not a proper boundary condition at the other end: if c and d were unequal there would obviously be no solution, while if c and d were equal there might be infinitely many solutions (depending on the other boundary conditions), as one of the integration constants is not fixed. In either case the BVP is said to be ill-posed. Another, independent, boundary condition needs to be imposed instead to obtain a locally unique solution (i.e., a solution with no infinitesimally close solutions, meaning that it is the only solution in an infinitesimal neighbourhood but that there may be additional solutions further away). It is not always a priori clear that a given ODE has one or several conserved quantities and well-posedness of a BVP is generally not straightforward.

Conserved quantities can be viewed as continuous symmetry properties of the ODE. A more obvious example of continuous symmetry is rotational symmetry of the equations, in which case for a well-posed BVP one has to impose boundary conditions that break the symmetry, thereby picking out one of the continuous family of solutions. Besides continuous symmetry a BVP may also have discrete symmetry, for instance reflection symmetry, in which case the BVP has multiple *isolated*

solutions. An example is the buckling of a ruler under compression, with the ruler deflecting either 'up' or 'down'. Nonlinear problems generally may have multiple, isolated, solutions. Each of such isolated solutions will generally be locally unique and the BVP is considered well-posed, with the solution being *globally* non-unique. Conserved quantities do not necessarily distinguish between such isolated solutions. This paper is mainly concerned with local non-uniqueness, not with this global non-uniquenesss, which only occurs in nonlinear problems.

3 Equilibrium equations for an elastic whisker

We model the whisker as a Kirchhoff rod. This is a geometrically exact elastic model suitable for slender structures undergoing large deformations.

Let xyz be an orthogonal laboratory frame fixed at the base of the whisker (see Fig. 1). The whisker is taken to be inextensible and unshearable and to have length L. Its thickness is neglected and its centreline is denoted by $\mathbf{r}(s) = (x(s), y(s), z(s))$, where $s \in [0, L]$ is arclength along the whisker, $s = 0$ corresponding to the base and $s = L$ corresponding to the tip.

Under the above assumptions we can introduce a local orthonormal material frame $\{\mathbf{d}_1, \mathbf{d}_2, \mathbf{d}_3\}$ along the length of the whisker, with $\mathbf{d}_1$ tangent to the centreline $\mathbf{r}$, i.e.,

$$\mathbf{r}' = \mathbf{d}_1,$$

and $\mathbf{d}_2$ and $\mathbf{d}_3$ directed along principal axes of the whisker's cross-section (here and in the following a prime denotes differentiation with respect to s). By orthonormality of the material frame there exists a (Darboux) vector $\mathbf{\Omega}$ such that

$$\mathbf{d}_i' = \mathbf{\Omega} \times \mathbf{d}_i \qquad (i = 1, 2, 3).$$

The components of this vector in the material frame, $(\omega_1, \omega_2, \omega_3) =: \boldsymbol{\omega}$, $\omega_i = \mathbf{\Omega} \cdot \mathbf{d}_i$, are the strains of the theory, i.e., the curvatures ω_2 and ω_3, about $\mathbf{d}_2$ and $\mathbf{d}_3$, and the twist ω_1, about $\mathbf{d}_1$ [10, 19].

The force and moment balance equations for the whisker can be written as

$$\mathbf{F}' + \boldsymbol{\omega} \times \mathbf{F} = \mathbf{0}, \tag{1}$$

$$\mathbf{M}' + \boldsymbol{\omega} \times \mathbf{M} + \mathbf{i} \times \mathbf{F} = \mathbf{0}, \tag{2}$$

where $\mathbf{F} = (F_1, F_2, F_3)$ and $\mathbf{M} = (M_1, M_2, M_3)$ are triples of force and moment components in the material frame and $\mathbf{i} = (1, 0, 0)$ (this being the tangent vector $\mathbf{r}'$ expressed in the material frame).

Finally, we assume linear elastic behaviour and specify the following constitutive relations, relating the moments to the strains:

$$M_1 = C(s)\omega_1,$$
$$M_2 = B(s)\omega_2, \quad M_3 = B(s)(\omega_3 - \omega_{30}(s)).$$

Figure 1 Whisker in point contact with an object at $s = s^*$. For frictionless contact the contact force is normal to the whisker and given by $F_n = \sqrt{F_2^2 + F_3^2}$.

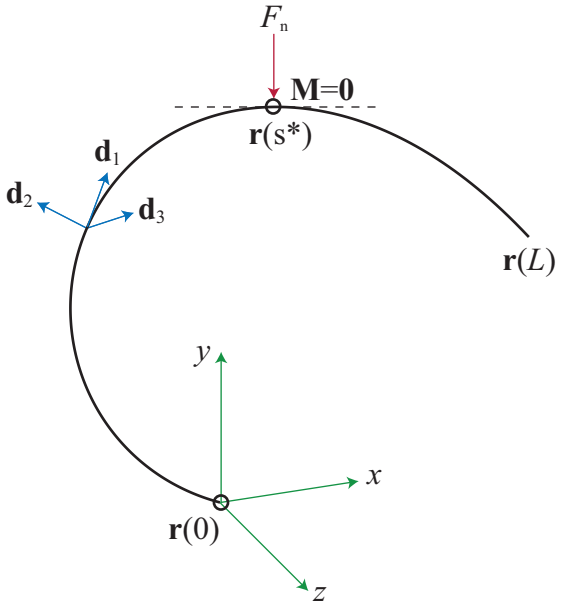

Here, $B(s)$ and $C(s)$ are the bending and torsional stiffnesses, respectively, which both may vary with arclength s (as, for instance, in a tapered whisker), but the stiffnesses for bending about $\mathbf{d}_2$ and $\mathbf{d}_3$ are identical. The undeformed shape of the whisker is taken to be planar with (possibly zero) intrinsic curvature $\omega_{30}(s)$. Extension of the model to allow for unequal bending stiffnesses or non-planar intrinsic curvature is straightforward, but most whiskers have symmetric cross-sections and are planar in their unstressed state [20].

We are interested in whisker configurations with a single (unknown) contact point at $s = s^\star \le L$ (see Fig. 1). It is convenient to introduce a scaled independent variable $\sigma = s/s^\star$, $\sigma \in [0, 1]$. The full system of equilibrium equations can then be written as

$$\begin{aligned}
\frac{d\mathbf{r}}{d\sigma} - \ell\,\mathbf{d}_1 &= \mathbf{0},\\
\frac{d\mathbf{d}_i}{d\sigma} - \ell\,\boldsymbol{\omega} \times \mathbf{d}_i &= \mathbf{0},\\
\frac{d\mathbf{F}}{d\sigma} + \ell\,\boldsymbol{\omega} \times \mathbf{F} &= \mathbf{0},\\
\frac{d\mathbf{M}}{d\sigma} + \ell\,\boldsymbol{\omega} \times \mathbf{M} + \ell\,\mathbf{i} \times \mathbf{F} &= \mathbf{0},\\
\frac{d\ell}{d\sigma} &= 0,
\end{aligned} \tag{3}$$

where ℓ is introduced as an auxiliary dependent variable subject to the boundary condition $\ell(1) = s^*$. Taking into account that the frame $\{\mathbf{d}_1, \mathbf{d}_2, \mathbf{d}_3\}$ is orthonormal and therefore defined by three independent components (we could for instance parametrise it by means of three Euler angles [10, 19]), this constitutes an ODE of order 13.

The system (3) has a number of conserved quantities [19, 21]. Eqs (1) and (2) imply, respectively, that $\mathbf{F}\cdot\mathbf{F}$ and $\mathbf{F}\cdot\mathbf{M}$ are constant. Further conserved quantities exist in special cases. If the whisker is intrinsically straight ($\omega_{30}\equiv 0$) then the twisting moment M_1 is constant as a result of rotational symmetry about the whisker's centreline. Lastly, a special role is played by the quantity

$$H=\frac{1}{2}\left(\frac{M_1^2}{C}+\frac{M_2^2+M_3^2}{B}\right)+M_3\omega_{30}+F_1, \tag{4}$$

called the Hamiltonian (in an appropriate Hamiltonian formulation of rod mechanics [21]). This H, which does not have a direct physical interpretation, is a conserved quantity provided B, C and ω_{30} are constant.

We assume the whisker to be fixed in both position and orientation at the base ($\sigma=0$). At the contact point ($\sigma=1$) a contact force will act from the surface of the object onto the whisker. In the case of frictionless contact this force will be normal to the surface and hence also normal to the whisker's centreline, thus $F_1(1)=0$. We will in addition make the common assumption that there is no contact (bending or twisting) moment, i.e., $\mathbf{M}(1)=\mathbf{0}$, which is consistent with neglecting whisker thickness.

We therefore consider the following 13 boundary conditions for system (3):

$$\begin{aligned}\mathbf{r}(0)&=\mathbf{0}, & \mathbf{M}(1)&=\mathbf{0},\\ \mathbf{d}_i(0)&=\mathbf{d}_{i,0}, & F_1(1)&=0,\\ \mathbf{P}(0)&=\mathbf{P}_0,\end{aligned} \tag{5}$$

where $\mathbf{P}=(P_1,P_2,P_3)$ is the vector of base measurements consisting of three components chosen from the six force and moment components F_1,F_2,F_3,M_1,M_2,M_3.

We note that three base measurements are sufficient for the well-posedness of the tactile sensing BVP (3)+(5), as also concluded in [15]. In Section 4 we analyse how this well-posedness depends on the precise choice of measured components P_i. For this, following [15], we also introduce polar representations of the force and moment in the whisker. Thus we write $F_2=F_n\cos\alpha$, $F_3=F_n\sin\alpha$, $M_2=M_n\cos\beta$, $M_3=M_n\sin\beta$. Here $F_n=\sqrt{F_2^2+F_3^2}$ and $M_n=\sqrt{M_2^2+M_3^2}$ are the magnitudes of the normal force and moment components, while α and β are the angles these components make with the material axes. We then have

$$\begin{aligned}\mathbf{F}\cdot\mathbf{F}&=F_1^2+F_n^2=\text{const},\\ \mathbf{F}\cdot\mathbf{M}&=F_1M_1+F_nM_n\cos(\alpha-\beta)=\text{const}=0,\end{aligned} \tag{6}$$

while the Hamiltonian (4) becomes

$$H=\frac{1}{2}\left(\frac{M_1^2}{C}+\frac{M_n^2}{B}\right)+M_n\omega_{30}\sin\beta+F_1. \tag{7}$$

Considering the six quantities $F_1,F_n,\alpha,M_1,M_n,\beta$ as possible independent measurements (as an alternative to the six independent components F_1,F_2,F_3,M_1,M_2,M_3) in Section 4 will give further insight into the sensing problem even though it is not immediately clear how in practice one could have direct access to, for instance, F_n without first measuring the material-frame components F_2 and F_3.

4 Analysis of the three-dimensional case

4.1 Intrinsically straight whiskers

For an intrinsically straight whisker ($\omega_{30}=0$), the boundary condition $M_1(1)=0$, together with the fact that M_1 is conserved, implies that the whisker remains twistless. It will consequently adopt a planar configuration (lying in a plane containing the $\mathbf{d}_{1,0}$ axis). Thus, if the base boundary conditions include the specification of the twisting moment M_1 (i.e., if one of the P_i equals M_1) then the BVP (3)+(5) is ill-posed. It will in general not have a unique solution, which means that the location of the contact point cannot be inferred from the base measurements $\mathbf{P}$. The last is also true if both α and β are included in $\mathbf{P}$, because (6) implies $\cos(\alpha-\beta)=0$, unless F_n or M_n is zero, which is true only in very exceptional cases (for instance, if the contact force is in the direction of the base tangent $\mathbf{r}'(0)$).

If the whisker has constant cross-section so that B and C are constant, then H is constant. The right-end boundary conditions imply that $H=0$ (in addition to $M_1=0$). Referring to (4), it then follows that $\mathbf{P}$ cannot equal (F_1,M_2,M_3) for a unique solution since the three components are not independent. In addition, referring to (7), we see that $\mathbf{P}$ cannot include both F_1 and M_n, independent of the third measurement (the two cases are of course equivalent if measuring M_n requires measuring M_2 and M_3).

All other choices for $\mathbf{P}$ will generically yield a (locally) unique solution and can therefore be used to predict the location of the contact point for an intrinsically straight whisker, with or without constant cross-section, but rare obstructions to uniqueness and hence predictability may occur as discussed in Section 2.

4.2 Intrinsically curved whiskers

For an intrinsically curved whisker M_1 is not a conserved quantity and hence $M_1(0)$ is not implied by the right-end boundary conditions in (5). Thus, whether or not the Hamiltonian is conserved, it will pose no constraint on the values of $\mathbf{P}(0)$, and neither will $\mathbf{F}\cdot\mathbf{M}$. Generically, any choice for $\mathbf{P}$ can be used to determine the location of the contact point.

An intrinsically curved whisker in general will adopt a non-planar configuration. This is true even if the whisker is intrinsically planar: the contact force will generally push the whisker out of its plane of intrinsic curvature. In exceptional cases, however, an intrinsically curved whisker may happen to be deformed into a planar configuration. The whisker is then necessarily

Table 1 Triples $\mathbf{P}$ of Cartesian measurements that give rise to an ill-posed BVP, and therefore a non-unique solution, for various intrinsic shapes of the rod (* stands for any of the other quantities and × indicates that there are no triples giving non-unique solutions).

rod	cylindrical ($B, C = \text{const.}$)	tapered ($B, C \neq \text{const.}$)
straight ($\omega_{30} = 0$)	$(M_1, *, *)$ (F_1, M_2, M_3)	$(M_1, *, *)$
curved ($\omega_{30} \neq 0$)	×	×

twistless and therefore $M_1(0) = 0$. Since the whisker is intrinsically curved, the plane will necessarily be the plane of intrinsic curvature. This means that $\alpha = 0$ (or π) and $\beta = \pm\pi/2$. We conclude that $\mathbf{P}$ cannot include M_1 but that Eq. (6) does not give any further constraint. If H is conserved (i.e., if B, C and ω_{30} are constant) then $\mathbf{P}$ cannot equal (F_1, M_2, M_3) or include both F_1 and M_n, by the same argument as in Section 4.1. Section 5 gives a detailed genuinely planar analysis of this exceptional case.

4.3 Summary of results

The results of our analysis are summarised in Tables 1 and 2 for Cartesian and polar components respectively, where those combinations of force/moment measurements are listed that are not appropriate in the design of an effective set of sensors at the base of a robotic whisker. A tapered whisker may here be interpreted as any whisker whose B or C is not constant.

5 Planar whisker configurations

In Section 4.1 we found that intrinsically straight whiskers always adopt a planar configuration in the present tactile sensing problem, but that the precise orientation of the plane is a priori unknown. By contrast, according to the analysis in Section 4.2, intrinsically curved whiskers may or may not deform into a planar configuration, but if they do then the orientation of the plane is determined by the plane of intrinsic curvature. If the whisker shape is planar, *and we know in which plane it lies*, then a strengthened analysis can be given.

Table 2 Triples $\mathbf{P}$ of polar measurements that give rise to an ill-posed BVP (* stands for any of the other quantities and × indicates that there are no triples giving non-unique solutions).

rod	cylindrical ($B, C = \text{const.}$)	tapered ($B, C \neq \text{const.}$)
straight ($\omega_{30} = 0$)	$(M_1, *, *)$ $(\alpha, \beta, *)$ $(F_1, M_n, *)$	$(M_1, *, *)$ $(\alpha, \beta, *)$
curved ($\omega_{30} \neq 0$)	×	×

Assuming that the whisker lies in the xy-plane, we may set $z \equiv 0$, $\mathbf{d}_3 \equiv (0, 0, 1)$, $\omega_1 \equiv \omega_2 \equiv 0$ (hence, $M_1 \equiv M_2 \equiv 0$) and $F_3 \equiv 0$ (i.e., $\alpha \equiv 0$, $\beta \equiv \pi/2$). The frame $\{\mathbf{d}_1, \mathbf{d}_2, \mathbf{d}_3\}$ now has only one angular degree of freedom and C is no longer relevant. Setting $\mathbf{d}_1 = (\cos\theta, \sin\theta, 0)$, θ being the angle the tangent makes with the x axis, system (3) reduces to the following 7th-order system for the remaining non-zero variables:

$$\begin{aligned}
\frac{dx}{d\sigma} - \ell\cos\theta &= 0,\\
\frac{dy}{d\sigma} - \ell\sin\theta &= 0,\\
\frac{d\theta}{d\sigma} - \ell\left(\frac{M_3}{B} + \omega_{30}\right) &= 0,\\
\frac{dF_1}{d\sigma} - \ell F_2\left(\frac{M_3}{B} + \omega_{30}\right) &= 0,\\
\frac{dF_2}{d\sigma} + \ell F_1\left(\frac{M_3}{B} + \omega_{30}\right) &= 0,\\
\frac{dM_3}{d\sigma} + \ell F_2 &= 0,\\
\frac{d\ell}{d\sigma} &= 0.
\end{aligned}$$

In [7, 9] this system is solved with a complete set of initial conditions at $\sigma = 0$. However, continuing with our assumption that the contact point is unknown, the two-point boundary conditions (5) reduce to

$$\begin{aligned}
x(0) &= 0, & M_3(1) &= 0,\\
y(0) &= 0, & F_1(1) &= 0,\\
\theta(0) &= \theta_0,\\
\mathbf{P}(0) &= \mathbf{P}_0, & &
\end{aligned} \tag{8}$$

where the vector of base measurements $\mathbf{P} = (P_1, P_2)$ now contains two components chosen from the three force and moment components F_1, F_2, M_3.

The Hamiltonian is now given by

$$H = \frac{M_3^2}{2B} + M_3\omega_{30} + F_1. \tag{9}$$

The boundary conditions (8) imply that for a cylindrical whisker with constant (possibly zero) intrinsic curvature, $H = 0$. It follows that if we choose to measure $F_1(0)$ and $M_3(0)$ then no unique solution will generically be obtained, since the boundary conditions are constrained by the value of H, but that the other (two) choices in general yield a unique solution and can therefore be used to determine the location of the contact point.

If the whisker has a non-uniform cross-section and/or varying intrinsic curvature, then H is not constant and therefore provides no constraint on the boundary conditions. Any combination of base measurements will

Table 3 Pairs **P** of measurements giving a non-unique solution for planar whisker configurations (× indicates that there are no pairs giving non-unique solutions).

rod	cylindrical ($B = \text{const.}$)	tapered ($B \neq \text{const.}$)
constant ω_{30}	(F_1, M_3)	×
non-constant ω_{30}	×	×

generically yield a unique solution. Table 3 summarises the results for planar whisker configurations.

Note that these results of the planar analysis are entirely consistent with the 3D analysis in Section 4.1, where no a priori knowledge of the plane was assumed, if we take into account that one extra boundary condition is needed to determine the plane of the whisker (for instance, from measurement of $M_2(0)$ and $M_3(0)$ the plane can be deduced). The results also agree with (and in fact explain) the numerical findings of section 2(f) in [12] for straight cylindrical and tapered whiskers. In particular, the graph in Fig. 2(f) is precisely a plot of Eq. (9) for $H = 0$ (and $\omega_{30} = 0$). The condition $H = 0$ is also noted in [22] for whiskers of constant intrinsic curvature.

6 Tip contact

In the special case of tip contact the object exerts an *unknown* axial force on the whisker (in addition to a normal force). The boundary condition $F_1(1) = 0$ must therefore be dropped. However, since the location of the contact point is now known, $\ell = s^\star = L$, the last equation in (3) can also be dropped. So for a well-posed BVP we still require three base measurements. Considering the (frictionless) case, in which H is conserved, the constant value of H is then no longer fixed at the right end ($\sigma = 1$) and H therefore poses no obstruction to obtaining a (locally) unique solution (in either the 3D or 2D formulation). This solution can for instance be used to determine the reaction force $F_1(1)$. This force will generally be nonzero, hence the value of H will be nonzero in the case of tip contact. It follows that by measuring the value of the Hamiltonian at the base one can establish whether the whisker makes interior-point contact or tip contact with an object (as also observed in [22, 17]).

A base sensor for predicting the location of point contact, that would be able to handle both tip and non-tip contact without assuming either, could therefore be based on the following procedure, valid only for whiskers for which the Hamiltonian H is conserved (i.e., whiskers with constant B, C and ω_{30}). First measure the three quantities M_2, M_3 and F_1, and from them, together with $M_1 = 0$, compute H. If $H = 0$ (signalling non-tip contact) then we solve (3) subject to the boundary conditions (5) with an appropriate triple of base measurements. According to Table 1, for a whisker with $\omega_{30} \neq 0$ the measured triple is appropriate and allows the contact point to be determined. If $\omega_{30} = 0$, however, then an extra, fourth, base measurement (either F_2 or F_3) has to be performed. If $H \neq 0$ (signalling tip contact) then we drop the last equation in (3) and the last boundary condition in (5). Whether or not $\omega_{30} = 0$, the measured triple is now acceptable, so no further base measurement is required. In the planar case we need only measure M_3 and F_1 to compute H. For tip contact these two measurements determine the location of the contact point. For non-tip contact, however, an extra, third, base measurement (F_2) is required.

7 Multiple point contact

The analysis of single point contact in the previous sections can be extended to whisker configurations with multiple frictionless point contacts provided the number of such contacts may be assumed known. Along whiskers with additional interior point contacts, all quantities in equation (3) are continuous except for the force $\mathbf{F}$, which is only continuous (and constant) between point contacts, where the normal (shear) component $F_2\mathbf{d}_2 + F_3\mathbf{d}_3$ of the force makes a jump in the direction of the contact point on the surface of the rod [24].

We can therefore compute whisker configurations with multiple contacts, at say $s = s_i$, $i = 1, 2, ...$, by solving the system of equations (3) for each contact-free segment (scaled to $[0, 1] \ni \sigma$) while imposing $\ell(1) = s_i - s_{i-1}$, $s_0 = 0$, and continuity conditions on all other variables, except for F_2 and F_3, at each contact point between two segments, and the boundary conditions (5) divided between the first and the last segment. Thus for each additional interior point contact there are three further unknowns, s_i (i.e., $\ell(1)$), $F_2(1)$ and $F_3(1)$, that need to be resolved, by adding boundary conditions at the whisker base, in order to be able to predict the location of all contact points. This means that two non-tip point contacts require six base measurements, while three or more non-tip contacts cannot be resolved by base measurements alone (of which there are only six possible). Since all components F_i, M_i are now included in the base measurements we have lost our ability to predict the location of multiple contact points from base measurements, except for those types of whisker against which a × appears in Tables 1, 2 or 3 (and for two contacts only). The conclusions of this paragraph also apply if the last of the multiple contacts is tip contact.

In the planar case, each interior point contact introduces two unknowns, s_i and the normal force component F_2 at s_i. There are, however, only three base measurements possible so we cannot resolve two-point contact. This confirms and explains preliminary observations made in [17]. The result holds for both tip and non-tip contact.

8 Discussion

We have highlighted the role of conserved quantities in whether or not a BVP for an ODE is well-posed in the sense that it has an isolated, i.e., locally unique, solution. If the boundary conditions at one end are such that they fix the value of a conserved quantity, then this quantity may constrain the choice of boundary conditions at the other end. A conserved quantity in this situation where it poses a constraint may be called *active*. We have shown that in the BVP for the (non-tip) contact problem of a (animal or robotic) whisker in tactile sensing, active conserved quantities constrain the choice of force and moment measurements, of which three are required (for tip contact no such constraint occurs).

Explicitly, our analysis has revealed that the twisting moment M_1 is an active conserved quantity for tactile sensing with an intrinsically straight whisker that has equal bending stiffnesses about the two principal directions ($\mathbf{d}_2$ and $\mathbf{d}_3$) of its cross-section. For such whiskers the conserved quantity $\mathbf{F}\cdot\mathbf{M}$ (i.e., the moment about the contact force) is additionally active for direct measurement of the directions, α and β, of the normal force and moment (supposing this is technically possible). The Hamiltonian H is an active conserved quantity, again additional to M_1, if the whisker is cylindrical. Consequently, for such whiskers some combinations of the three base measurements do not allow the determination of the contact point. Tables 1 and 2 list all triples, of Cartesian and polar components respectively, that give rise to non-unique solutions and therefore should be avoided when designing robust sensors at the base of a robotic whisker [16, 23]. For completeness, Table 3 lists pairs of base measurements that should be avoided in the planar tactile sensing problem. Mammal whiskers, however, are usually tapered and intrinsically curved and for them no such obstruction occurs.

Statements on the uniqueness of a solution of a BVP for a nonlinear ODE are only valid locally and generically, i.e., away from any special (bifurcation) parameter values. Multiple solutions occur, for instance, in problems with reflection symmetry, elastic buckling under axial loads being an example. These solutions are usually isolated, in which case the analysis of this paper applies locally to each of them individually. In most sensing applications local uniqueness will likely be sufficient, with 'context' providing clues as to which of several global alternatives one is dealing with.

The complete test of non-uniqueness of the pairing between contact point position $\mathbf{r}(1)$ and base measurements $\mathbf{P}(0)$ may be carried out by numerically integrating the BVP (3)+(5) for a range of values for the chosen triple $\mathbf{P}$ and recording the corresponding values of $\mathbf{r}(1)$. However, a more economical approach, that avoids having to solve the problem for 20 different combinations of triples $\mathbf{P}$, would be to specify the position $\mathbf{r}(1)$ instead and to solve equation (3) with boundary conditions

$$\begin{aligned} \mathbf{r}(0) &= \mathbf{0}, & \mathbf{r}(1) &= \mathbf{r}_1, \\ \mathbf{d}_i(0) &= \mathbf{d}_{i,0}, & \mathbf{M}(1) &= \mathbf{0}, \\ & & F_1(1) &= 0 \end{aligned} \tag{10}$$

for a mesh of accessible values of $\mathbf{r}_1$ in physical space. The solutions to (3) and (10) give all the base forces and moments, from which any triple can be selected. For a chosen triple $\mathbf{P}$ one can then consider the map $S:\mathbf{r}_1\mapsto\mathbf{P}_0$ and evaluate its 3×3 Jacobian matrix $\frac{\partial\mathbf{P}_0}{\partial\mathbf{r}_1}$ at a computed solution. If the determinant of this matrix is zero then we have local non-uniqueness, otherwise local uniqueness. Eigenvectors of $\frac{\partial\mathbf{P}_0}{\partial\mathbf{r}_1}$ give measures for the relative sensitivity in the various quantities of the particular triple, which could be considered in sensor design.

A comprehensive numerical study is beyond the scope of this paper, but we computed the determinant in this way for a few randomly chosen data for all 20 combinations of the force/moment triples and for all four combinations of straight/curved and cylindrical/tapered whiskers. All results are in agreement with the analysis in Section 4.

Our analysis of active conserved quantities helps explain numerical observations on contact point predictability in the literature. Table 3 explains all reports of non-uniqueness in [12] for the 2D sensing problem. For the 3D problem, [15] lists results for all 20 cases of base triples $\mathbf{P}(0)$ in cylindrical coordinates. Tables 1 and 2 explain all reports of non-uniqueness in Table 2 of [15] for intrinsically straight whiskers except for tapered ones in Case 7. For intrinsically curved whiskers our Tables 1 and 2 are consistent with all results in Table 2 of [15] but do not explain reports of non-uniqueness for Cases 7, 16, 17, 19 and 20. In the following paragraphs we discuss these exceptional cases further.

Non-uniqueness in Case 7 (F_1, M_n, F_n) for straight whiskers (tapered or cylindrical) can be explained by noting that the deformed whisker configuration is planar but that the base measurements do not include an angle and therefore the orientation of the plane is not determined. The whisker can lie in any plane through the $\mathbf{d}_{1,0}$ axis. Since the contact point need not lie on this axis, the same base triple $\mathbf{P}_0$ corresponds to multiple $\mathbf{r}_1$ and the map S is therefore non-injective. This is an example of continuous (namely rotational) symmetry and the non-uniqueness is local.

Case 7 for curved whiskers can be explained by discrete symmetry. The equations (3) are invariant under the following symmetry transformation (involution): $F_1\leftrightarrow F_1$, $F_2\leftrightarrow F_2$, $F_3\leftrightarrow -F_3$, $M_1\leftrightarrow -M_1$, $M_2\leftrightarrow -M_2$, $M_3\leftrightarrow M_3$. This transformation corresponds to reflection of the solution in the $(\mathbf{d}_{1,0},\mathbf{d}_{2,0})$ plane. Now since in Case 7 no angular information is obtained at the whisker base, measurement cannot distinguish between any two symmetrically related solutions. This means that for 3D whisker configurations with contact point not lying in the $(\mathbf{d}_{1,0},\mathbf{d}_{2,0})$ plane (i.e., $\mathbf{r}(1)\cdot\mathbf{d}_{3,0}\neq 0$)

the base triple $\mathbf{P}_0$ corresponds to two different contact points $\mathbf{r}_1$ and therefore the map S is non-injectivce. Note that, unlike the non-uniqueness caused by the existence of active conserved quantities, this non-uniqueness due to discrete symmetry is a global non-uniqueness; it is not detected by the determinant test described above. (This discrete symmetry also highlights a subtle distinction between non-uniqueness of solutions of the BVP and non-injectivity of the map S: if the BVP has non-planar solutions all of which happen to satisfy $\mathbf{r}(1) \cdot \mathbf{d}_{3,0} = 0$ then by virtue of the above symmetry it has no unique solution, but the map S is injective because all symmetrically related solutions have the same contact point.)

It is worth noting that both these instances of non-uniqueness in Case 7, local and global, would have been avoided by working with Cartesian components: if Cartesian measurements F_i, M_i had been used there would have been no sign degeneracy and one would generically have expected injectivity of the map S.

For the other four exceptional Cases 16, 17, 19 and 20 we can only suggest that some similar global non-uniqueness, with isolated solutions, was found in [15], a non-uniqueness that, unlike in Case 7, is not explained by an obvious symmetry. Cases 16, 17, 19 hint at this by having different predictions for tapered and cylindrical curved rods, which is hard to explain otherwise. As our analysis, based on conserved quantities, is local, we cannot make any general claims about global non-uniqueness, and [15] does not give details on the precise nature of the observed non-uniqueness (e.g., whether or not the solutions are isolated). For planar configurations, however, the reported non-uniqueness in Cases 16 and 17 is clear because the measurements include only one meaningful quantity, F_1, while two are required for uniqueness (the same lack of meaningful measurements explains all the cases labelled by an asterisk in Table 2 of [15]). Case 19 is also clear for planar configurations because its two meaningful measurements, F_1 and M_3, are inappropriate for unique prediction according to Table 3. It is notable that the four exceptional cases are the cases $(F_1, M_1, *)$, with * any of the four polar components. To demonstrate that it is possible to *construct* isolated pairs of solutions with identical base triples, in the Appendix we give details of two distinct non-planar solutions with the same values of $M_1(0)$, $F_1(0)$ and $F_2(0)$. Such pairs are accidental though and could easily be missed in numerical searches as in [15].

Although our results have been obtained within the context of geometrically-exact rod theory, our analysis has been entirely qualitative and would equally apply to any other 1D (hyper)elastic theory. This extends to the existence of conserved quantities, which are consequences of the fundamental laws of mechanics. Indeed, the equations (3) could be considered a 'black box' holding a 1D elastic medium that connects inputs at $\sigma = 1$ to outputs at $\sigma = 0$. If another mechanical model were used (e.g., a beam model only allowing for small deformations or a model also including shearability or extensibility of the whisker or a nonlinearly elastic rod model) then different whisker shapes and different forces and moments might be computed but the predictability or otherwise of the contact point position from base measurements would be unaltered. Thus all the above statements of local non-uniqueness based on conserved quantities or continuous symmetry and global non-uniqueness based on discrete symmetry, which are all independent of model details, would remain valid. By contrast, statements of global non-uniqueness for the exceptional Cases 16, 17, 19 and 20 of [15] would likely be conditional on model details.

In a real laboratory situation M_1 or H will never be found to be exactly zero. However, if they are nearly zero then this will significantly reduce the accuracy with which the location of the contact point can be predicted and it would be better to change the base measurements. If H as given in (4) (for a whisker with constant B, C and ω_{30}) is found to deviate significantly from zero then this points to a model error: some effect, for instance friction at the contact point, has not been included in the mathematical formulation.

In addition to M_1, $\mathbf{F} \cdot \mathbf{M}$ and H, the quantity $\mathbf{F} \cdot \mathbf{F}$ is conserved for an elastic rod, in fact independent of material and geometrical properties [21]. Its value, however, is not fixed at the contact point since F_2 and F_3 are generally not known there. This conserved quantity is therefore not active and provides no obstruction for the present tactile sensing BVP. It is also worth noting that if M_1 is not conserved (for instance for an intrinsically curved whisker, but also for a whisker with unequal principal bending stiffnesses) then $M_1(0)$ is not fixed and hence H depends on four unknown quantities ($M_1(0)$, $M_2(0)$, $M_3(0)$ and $F_1(0)$) and thus provides no constraint for three base measurements. Straight robotic whiskers could for instance be constructed with oval cross-section to avoid any obstruction to determining the location of the contact point through base measurements. It is good to realise though that when a whisker with non-circular cross-section makes contact with an object then generally a twisting moment will be induced, i.e., $M_1(1) \neq 0$, which changes the BVP. Assuming that no bending moments are induced, we then lose one of the boundary conditions at $\sigma = 1$ in (5) and therefore need an extra base measurement. Possible prediction of the position of the contact point would have to be re-examined for four base measurements, for which there are 15 combinations (quadruples of forces/moments).

Similarly, if contact is frictional then we no longer have $F_1(1) = 0$. Since friction will generally also induce a twisting moment $M_1(1)$, we in fact lose two right-end conditions and therefore need to impose two more left-end conditions, i.e., we require five base measurements, for which there are 6 combinations. Because $F_1(1)$ and $M_1(1)$ are now unknown, none of the conserved quantities is active in this case, so there is no obstruction to determining the location of the contact point through (five) base measurements. In case of only a small friction force, however, sensing accuracy would be

significantly degraded if these measurements included the combinations of Tables 1, 2 or 3, so it would still be prudent to avoid these cases.

For other rod problems different conserved quantities may be active, or different conserved quantities may exist (which may or may not be active). For example, the equilibrium equations for a conducting rod in a uniform magnetic field, relevant for electrodynamic tethers, has extra conserved quantities, involving the magnetic field, in addition to the standard rod Hamiltonian [21]. Our approach in this paper can be used to explore the implications of these extra conserved quantities for sensing applications using magnetically controlled whiskers.

Acknowledgement

The research is supported by the EPSRC grant EP/P030203/1 'MMEAW: Modelling the MEchanics of Animal Whiskers'.

References

[1] M. H. Evans, M. S. E. Loft, D. Campagner, and R. S. Petersen. Sensing the environment with whiskers, 2019. Oxford Research Encyclopedia, Neuroscience (oxfordre.com/neuroscience), Subject: Sensory Systems.

[2] K. Bagdasarian, M. Szwed, P. M. Knutsen, D. Deutsch, D. Derdikman, M. Pietr, E. Simony, and E. Ahissar. Pre-neuronal morphological processing of object location by individual whiskers. *Nature Neuroscience*, 16(5):622–631, 2013.

[3] L. Pammer, D. H. O'Connor, S. A. Hires, N. G. Clack, D. Huber, E. W. Myers, and K. Svoboda. The mechanical variables underlying object localization along the axis of the whisker. *Journal of Neuroscience*, 33(16):6726–6741, 2013.

[4] T. Pipe and M. J. Pearson. Whiskered robots, 2016. Scholarpedia of Touch, Scholarpedia.

[5] O. Bebek and M. C. Cavusoglu. Whisker-like position sensor for measuring physiological motion. *IEEE/ASME Transactions on Mechatronics*, 13(5):538–547, 2008.

[6] T. Tsujimura and T. Yabuta. Object detection by tactile sensing method employing force/torque information. *IEEE Transactions on Robotics and Automation*, 5(4):444–450, 1989.

[7] G. R. Scholz and C. D. Rahn. Profile sensing with an actuated whisker. *IEEE Transactions on Robotics and Automation*, 20(1):124–127, 2004.

[8] T. N. Clements and C. D. Rahn. Three-dimensional contact imaging with an actuated whisker. *IEEE Transactions on Robotics*, 22(4):844–848, 2006.

[9] L. Merker, C. Will, J. Steigenberger, and C. Behn. Object shape recognition and reconstruction using pivoted tactile sensors. *Mathematical Problems in Engineering*, 2018, 1613945, 2018.

[10] A. E. H. Love. *A Treatise on the Mathematical Theory of Elasticity*. Cambridge University Press, 1927.

[11] N. Ueno, M. M. Svinin, and M. Kaneko. Dynamic contact sensing by flexible beam. *IEEE/ASME Transactions on Mechatronics*, 3(4):254–264, Dec 1998.

[12] J. H. Solomon and M. J. Z. Hartmann. Radial distance determination in the rat vibrissal system and the effects of Weber's law. *Philosophical Transactions of the Royal Society B: Biological Sciences*, 366(1581):3049–3057, 2011.

[13] S. A. Hires, L. Pammer, K. Svoboda, and D. Golomb. Tapered whiskers are required for active tactile sensation. *eLife*, 2:e01350, 2013.

[14] S. Ahn and D. Kim. Radial distance estimation with tapered whisker sensors. *Sensors*, 17(7):1659, 2017.

[15] L. A. Huet, J. W. Rudnicki, and M. J. Z. Hartmann. Tactile sensing with whiskers of various shapes: Determining the three-dimensional location of object contact based on mechanical signals at the whisker base. *Soft Robotics*, 4(2):88–102, 2017.

[16] H. Emnett, M. Graff, and M. Hartmann. A novel whisker sensor used for 3D contact point determination and contour extraction. In *Proceedings of Robotics: Science and Systems*, Pittsburgh, Pennsylvania, June 2018.

[17] L. Merker, S. J. Fischer Calderon, M. Scharff, J. H. Alencastre Miranda, and C. Behn. Effects of multi-point contacts during object contour scanning using a biologically-inspired tactile sensor. *Sensors*, 20(2077), 2020.

[18] U. M. Ascher, R. M. M. Mattheij, and R. D. Russell. *Numerical Solution of Boundary Value Problems for Ordinary Differential Equations*. SIAM, Philadelphia, 1995.

[19] G. H. M. van der Heijden and J. M. T. Thompson. Helical and localised buckling in twisted rods: a unified analysis of the symmetric case. *Nonlinear Dynamics*, 21(1):71–99, 2000.

[20] E. L. Starostin, R. A. Grant, G. Dougill, G. H. M. van der Heijden, and V. G. A. Goss. The Euler spiral of rat whiskers. *Science Advances*, 6(3), 2020.

[21] D. Sinden and G. H. M. van der Heijden. Integrability of a conducting elastic rod in a magnetic field. *Journal of Physics A: Mathematical and Theoretical*, 41(4):045207, 2008.

[22] A. Sauter, Ch. Will, J. Steigenberger, and C. Behn. Artificial tactile sensors with pre-curvature for object scanning. In J. Awrejcewicz, M. Kazimierczak, J. Mrozowski, and P. Olejnik, editors, *Dynamical Systems: Mathematical and Numerical Approaches*, pages 425–436, 2015.

[23] D. W. Collinson, H. M. Emnett, J. Ning, M. J. Z. Hartmann, and L. C. Brinson. Tapered polymer whiskers to enable three-dimensional tactile feature extraction. *Soft Robotics*, 8(1):44–58, 2021.

[24] G. H. M. van der Heijden, S. Neukirch, V. G. A. Goss, and J. M. T. Thompson. Instability and self-contact phenomena in the writhing of clamped rods. *International Journal of Mechanical Sciences*, 45:161–196, 2003.

Appendix

The following graphs are three projections onto the coordinate planes and an axonometric projection of two deformed configurations ('red' and 'blue') of the same curved rod of length $L = 1$. The initial conditions for the forces and moments are:

red:

$$M_1(0) = -0.35, \quad M_2(0) = 8.314, \quad M_3(0) = 0.908,$$
$$F_1(0) = -35.0, \quad F_2(0) = 0.0, \quad F_3(0) = -21.913,$$

blue:

$$M_1(0) = -0.35, \quad M_2(0) = 4.968, \quad M_3(0) = -6.728,$$
$$F_1(0) = -35.0, \quad F_2(0) = 0.0, \quad F_3(0) = 1.731.$$

Both solutions satisfy the boundary conditions at the contact point: $M_i(s^*) = 0, i = 1, 2, 3, F_1(s^*) = 0$ at $s^* = 0.225$ (red) and $s^* = 0.325$ (blue). The coordinates of the contact point are:

red:	$x = 0.168,$	$y = -0.132,$	$z = -0.016,$
blue:	$x = 0.139,$	$y = -0.149,$	$z = 0.202.$

The intrinsic shape is a circular arc of radius $9/\pi$ (black) in the xz-plane (i.e., $\omega_{30} = \pi/9$). The bending and torsional stiffnesses are $B = 1.0$ and $C = 0.7$. Only the part of the centreline from the base to the contact point is shown. Arrows indicate the contact forces, which are chosen to be parallel to the xy-plane. Note that three initial components (M_1, F_1 and F_2) coincide for both solutions.